IEEE Photonics Journal
An IEEE Photonics Society Publication

Open Access

An Annulus-Sector Segmented Primary Mirror

Volume 9, Number 5, OCTOBER 2017

X. X. Wei
X. J. Wan
B. Yang

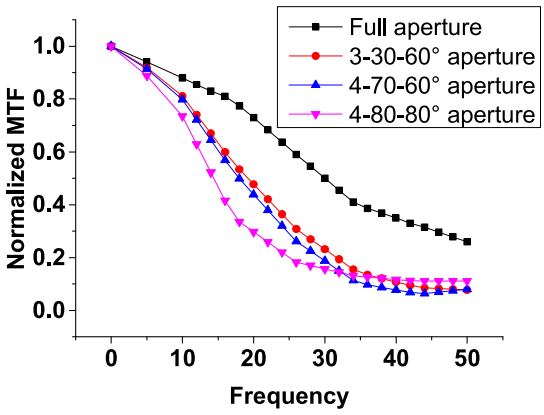

(a)

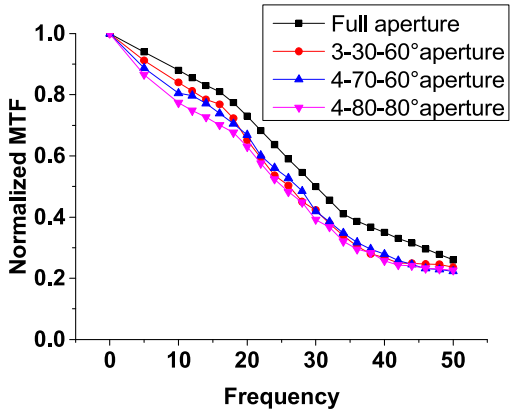

(b)

DOI: 10.1109/JPHOT.2017.2750705
1943-0655 © 2017 IEEE

IEEE photonics SOCIETY

IEEE

An Annulus-Sector Segmented Primary Mirror

X. X. Wei, X. J. Wan, and B. Yang

Shanghai Key Laboratory of Modern Optical System and Engineering Research Center of Optical Instrument and System, Ministry of Education, University of Shanghai for Science and Technology, Shanghai 200093, China

DOI:10.1109/JPHOT.2017.2750705

Manuscript received June 21, 2017; revised August 28, 2017; accepted September 6, 2017. Date of publication September 11, 2017; date of current version September 29, 2017. This work was supported in part by the Project of National Natural Science Foundation of China under Grants 61007010 and 61505107 and in part by the National Key Scientific Instrument Development Program 2012YQ17000403. Corresponding author: X. X. Wei (e-mail: weixx@usst.edu.cn).

Abstract: Ultrahigh resolution optical imaging with large aperture is increasingly desired in space-based remote sensing and imaging system, but it is usually limited by volume and mass constraints of launch vehicle due to size and weight of the imaging system. In this paper, an annulus-sector segment primary mirror is presented, which is in high obscuration with circularity symmetrical annulus-sector around. The different structure types of the annulus-sector segment aperture are discussed, while two important parameters, width–diameter ratio and the subaperture angle are also studied. An annulus-sector optical lens is processed to verify the image performance. Experimental results show that modulation transfer function of annulus-sector segment optical system can be up to 0.23(50 lp/mm), which approaches the optical resolution of full aperture optical system with smaller size and lighter weight.

Index Terms: Annulus-sector, segmented mirror, width-diameter ratio, sub-aperture angle, optical resolution.

1. Introduction

Large telescopes with ultra-high resolution is in high demand for both ground and space applications. An effective way to improve resolution is to increase the aperture diameter of the primary mirror. One of the well-known examples is the NASA's Next Generation Space Telescope (JWST), in which a 6.5-meter primary mirror is utilized and the optical angular resolution is expected to reach 0.1-arc-second [1], [2], [3]. The mass of the 6.5-meter primary mirror is, however, as heavy as 0.4 tons which creates a big challenge to launch. Moreover, it is less practical to scaling up the size of a conventional optical system in order to further increase the optical resolution, because the primary mirror diameter of such systems is limited by volume and mass constraints of launch vehicle as well as the manufacturing costs [4], [5]. To cope with these problems, an alternative is to use a sparse aperture, i.e., one with most of the aperture element missing. Many designs have been proposed, including annular, Golay, and tri-leg structures, which are based on Fizeau interferometer technique [6], [7], [8]. In contrast to the long baselines of Michelson interferometers, the Fizeau is suitable for optical imaging of extended objects and rapidly changing targets hence tend to have compact telescope arrays, especially the multiple mirror telescopes (MMT) [9], [10].

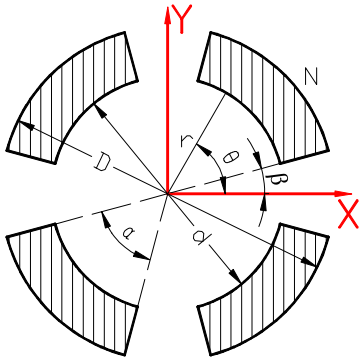

Fig. 1. The segmented primary mirror with N equals to 4.

The Giant Magellan Telescope (GMT), which is planned for completion in 2020, is a typical design to demonstrate the considerable performance of a large telescope by utilizing seven sparsely arranged mirrors (one mirror in the center and the other six arranged symmetrically around it), each 8.4 meters in diameter [11].

Variation in the types of sparse system or the arrangement of the sparse mirrors will result in different optical characteristics and functionality. To explore the capability and characteristics of more versatile and more practical sparse aperture system, the upcoming large astronomical telescopes are trending towards the Segmented Mirror Telescope (SMT) technology [12], [13], therefore, an annulus-sector segmented primary mirror which is designed to be highly obscuration with circularity symmetrical around is proposed in this paper. The proposed annulus-sector technique is to sparsely encode the primary aperture of large optics. Since it forms an intermediate blurring optical image on detector, the final sharp image is necessarily recovered with digital decode procedure. This technique combines optical design and digital image processing together so that substantial mass reduction of its large aperture primary and high imaging performance equivalent to its corresponding full-aperture optics can be concurrently implemented.

By introducing symmetric annulus-sector into the system, a larger field of view with larger depth of focus can be obtained. Furthermore, the outer annulus-sector segments are identical to each other. The prospect of assembling the primary mirror from small, low-cost identical spherical mirror segments is very attractive [14]. The manufacturing and testing of the segments can thus be easily realized without changing procedures. The annulus-sector primary mirror will be of significance because of its substantial mass reduction and still high imaging performance that is equivalent to full aperture one.

In this paper, the annulus-sector segmented primary mirror will be analyzed in detail, the optical properties will be presented by different types of structures, and then the main factors which affect the imaging performance are investigated. Furthermore, the image performance contrast between the annulus-sector and full aperture optical system are also studied, while an annulus-sector optical lens is processed to realize the imaging experiment.

2. Design of Annulus-Sector Primary Mirror

2.1 Structure of Segmented Primary Mirror

The illustration of the segmented primary mirror is presented in Fig. 1 and N is the pieces of segmented primary mirror. Considering that the angle of segment (α) is determined by the value of N, the relationship between α and N can be expressed by followings:

$$\alpha + 2\beta = \frac{2\pi}{\mathrm{N}} \tag{1}$$

Where β is the angle of segmented primary mirror deviating from the axis.

As is well known, the pupil function of ring structure can be expressed as [15]:

$$P_0(r,\theta) = circ\left(\frac{r}{D/2}\right) - circ\left(\frac{r}{d/2}\right) \tag{2}$$

For annulus-sector segmented structure, a step function (3) is introduced, the pupil function of annulus-sector primary mirror is deduced in formula (4).

$$\partial(\gamma) = \begin{cases} 1 & \gamma > 0 \\ 0 & \gamma \le 0 \end{cases} \tag{3}$$

$$P(r,\theta) = \left\{ circ\left(\frac{r}{D/2}\right) - circ\left(\frac{r}{d/2}\right) \right\} \cdot \sum_{n}^{N} \left\{ \partial\left(\theta - \left(\beta + \frac{2\pi(N-n)}{N}\right)\right) - \partial\left(\theta - \left(\alpha + \beta + \frac{2\pi(N-n)}{N}\right)\right) \right\} \tag{4}$$

Where $circ(\cdot)$ is circle function, $\partial(\cdot)$ is step function, d is the inner diameter of the segment primary mirror, and D is the outer diameter.

2.2 Analysis of Image Performance

The modulation transfer function (simplified MTF) is an important indicator to evaluate the image performance. As we know, the space optical system has no fixed observation target during observation, then the MTF is required to be continues response of spatial frequency. To preserve the full spatial frequency information, the MTF of annulus-sector pupil structure should be able to cover all the spatial frequencies that the external circle contains.

In annulus-sector structure design we consider two parameters to select the segmented pattern: width-diameter ratio ΔR and sub-aperture angle α, as shown in Fig. 1. The difference of two parameters has a critical effect on the imaging performance of annulus-sector pupil coded system.

Width-diameter ratio ΔR is the effective ring width to exradius, which can be expressed as followings:

$$\Delta R = \frac{D - d}{2D} \tag{5}$$

Where D is the outer diameter, d is the inner diameter, so $(D - d)/2$ is certainly the value of effective ring width.

To compare the MTF performance effect of annulus-sector optical system and that of full aperture, we consider a reflecting optical system, with focal length 1000 millimeter and aperture 100 millimeter, of which the annulus-sector structure is applied to the primary mirror. Take the segmented primary mirror with $N = 4$ and $\alpha = \pi/3$ for example, the width-diameter ratio ΔR are 0.5, 0.4, 0.3 and 0.2 respectively.

Fig. 2(a) depicts the different MTF performance between full aperture and annulus-sector aperture, we can see that as the width-diameter ratio ΔR decreases, the MTF at low and medium frequency decreases rapidly, but at high frequency, the changes are slow. When the width-diameter ratio is reduced from 0.5 to 0.2, the MTF at low and medium frequency decrease from 0.26 to 0.01, but the MTF at high frequency fell from 0.29 to 0.1.

It can be seen clearly from the chart that when the width-diameter ratio ΔR is lesser than 0.5, MTF of annulus-sector coded optical system presents to be flat at medium frequency and upward at high frequency. It suggests that MTF at high frequency is higher than that of full aperture system [16]. As a consequence, the annulus-sector structure with width-diameter ratio ΔR lesser than 0.5 will be discussed in the followings.

Still take the segmented primary mirror with $N = 4$ and $\Delta R = 0.4$ for example, the sub-aperture angle α is 30°, 45° and 60° respectively. Fig. 2(b) depicts the different MTF performance when the sub-aperture angle α changes, as α decreases, the MTF at low and medium frequency declines

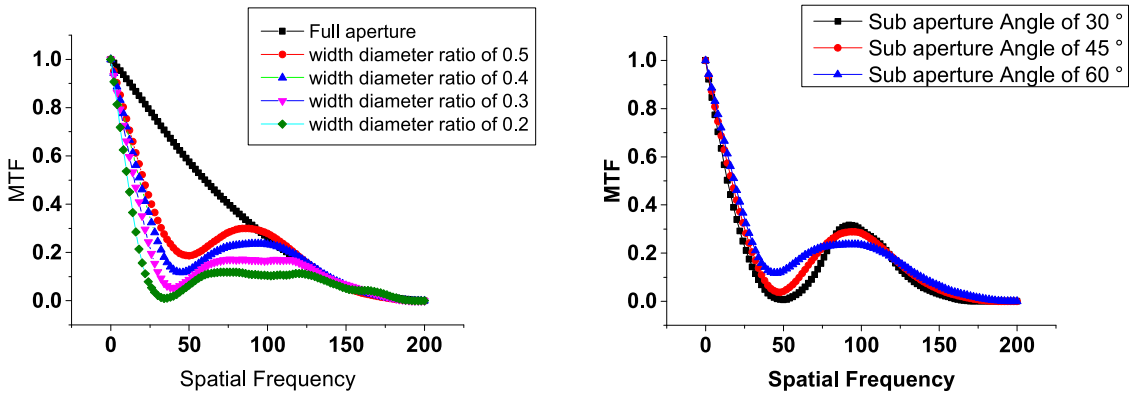

Fig. 2. Analysis of coded aperture system with different annulus-sector structure. (a) Full aperture vs. different width diameter ratio coded aperture. (b) Effect of different sub-aperture angle.

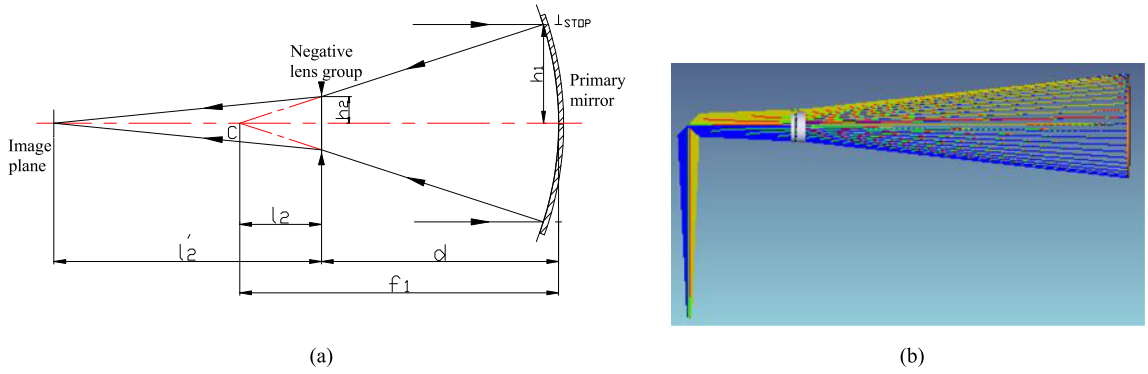

Fig. 3. Structure of catadioptric optical system. (a) Initial structure. (b) The design result in ZEMAX.

fast. When the value of α changes from 60° to 30°, the MTF at low and medium frequency decrease from 0.13 to zero, while the MTF at high frequency increases from 0.23 to 0.29. Based on the analysis above, the variation of sub-aperture angle α has a great influence on the MTF at low and medium frequency. We can see from Fig. 3(b) that when α equals to 30°, a zero-value area exists in the spatial frequency range, causing the target information to be lost. Although a lower of α makes a higher MTF at high frequency, in practice, the main target imaging is the low and medium frequency. Therefore, when the annulus-sector structure is being selected,it is necessary to make the appropriate tradeoff between two parameters, such as width-diameter ratio ΔR and sub-aperture angle α.

As we know, the increased aperture will make processing harder and larger weight. Therefore, the annulus-sector primary mirror can be divided into N pieces greater than 5, which reduces the processing difficulty to a large extent. Furthermore, the distortion of the segmented primary mirror is smaller than the full aperture, then the center thickness can be correspondingly decrease, which shows that the annulus-sector structure has a favourable and marked effect on light weight.

3. Image Experiment of Annulus-Sector Optical System and Results Discussion

3.1 Development of Annulus-Sector Optical System

To validate the imaging performance of annulus-sector segmented primary mirror, a catadioptric optical system is considered to be designed. The structure of catadioptric optical system is shown

in Fig. 3 (a). An object from infinity is reflected by primary mirror, which coincide with entrance pupil, and is magnified by the negative lens group to the image plane. The catadioptric optical system are particularly useful because of two key properties: (1) the primary mirror is spherical, which is convenient for processing with low cost; (2) the focal length of the primary does not need to be large and a long focal length optical system still can be obtained magnified by the negative lens group. The negative lens group is composed of two positive and negative lenses; the positive lens is flint glass with long focal length and the negative glass is crown glass with short focal length, which is good for chromatic aberration [17].

In general, the obstruction ratio caused by the negative lens group is expected to be small to reduce energy loss. In this design, the obstruction ratio is 0.3 and relative aperture of primary mirror is 1/4.5. Consequently, the initial structure of optical system can be determined by calculating the magnification and focal length of the negative lens group.

As shown in Fig. 3(a), the magnification m_B and focal length f_2 of the negative lens group can be calculated by following formulas:

$$m_B = \frac{f}{f_1} \tag{6}$$

$$\frac{h_2}{h_1} = \frac{l_2}{f_1} \tag{7}$$

$$l_2' = m \times l_2 \tag{8}$$

$$f = \frac{f_1 f_2}{f_1 + f_2 - d} \tag{9}$$

Where f_1 is the focal length of primary mirror, f is the focal length of system. h_1 is height of the entrance pupil, h_2 is the height of the lights enter the negative group. l_2 is the finite object distance of the negative group and l_2' is the corresponding image distance. d is the distance between the primary mirror and the negative group.

According to the above parameters, the optimized optical systems can be obtained in ZEMAX as shown in Fig. 3(b) with a plane mirror to turn the light. The focal length of optical system is 1000 mm, the aperture is 100 mm, and the optimized relative aperture of primary mirror is up to 1/4.43. The focal length of negative group f_2 is -231.8 mm and the magnification m_B is approximately 2.26. The image distance of negative group l_2' is 285 mm and the distance between the primary mirror and the negative group d is approximately 311.3 mm. Furthermore, the negative group is composed of a crown glass ZK11 and a flint glass F4, which is achromatic.

Through the distribution of tolerance, the structure design and processing, the spherical catadioptric optical lens is developed as shown in Fig. 4. MTF comparison between the designed and developed spherical catadioptric optical system is presented in Fig. 4(a). The designed MTF on axis at 50 lp/mm is up to 0.4 and the corresponding MTF of developed lens is 0.36. Considering the impact of tolerance, the developed spherical catadioptric optical lens shows a good optical performance.

3.2 Imaging Experiment of Annulus-Sector Optical Lens

We built an experimental device as shown in Fig. 5 to realize the imaging of annulus-sector optical lens. We used an AVT PIKE F-505C CCD sensor which offers a selection of six different high-quality sensors (b/w and color) with high sensitivity and true-to-life color reproduction. The sensor has 2452 $\times$ 2054 pixels, each 3.45 μm wide. The physical size of sensor is apporoximately 8.5 mm $\times$ 7.1 mm.

A collimator is used in this experimental program to produces infinitely parallel rays, the focal length of collimator is 2000 mm. The optical axis of collimator and optical lens is ensured to be consistent when imaging simulation.

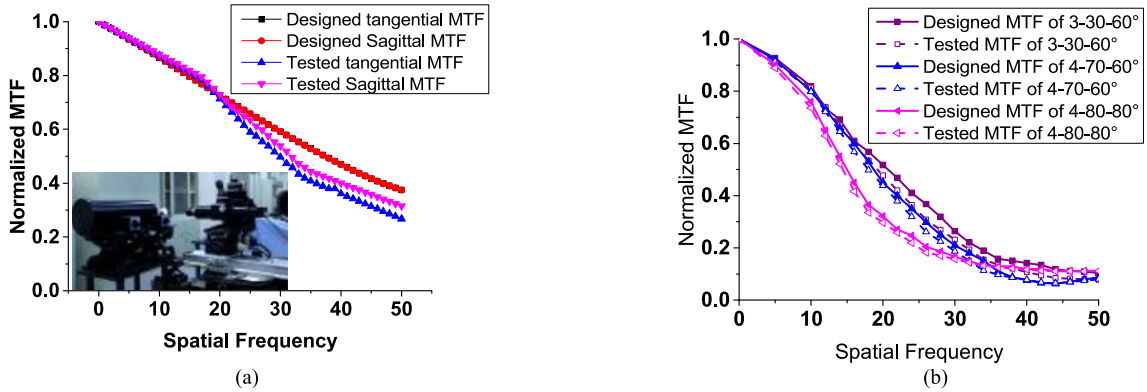

Fig. 4. MTF comparison of spherical catadioptric optical system. (a) Designed MTF VS Tested MTF of spherical catadioptric optical system. (b) Designed MTF VS Tested MTF of three annulus-sector structures.

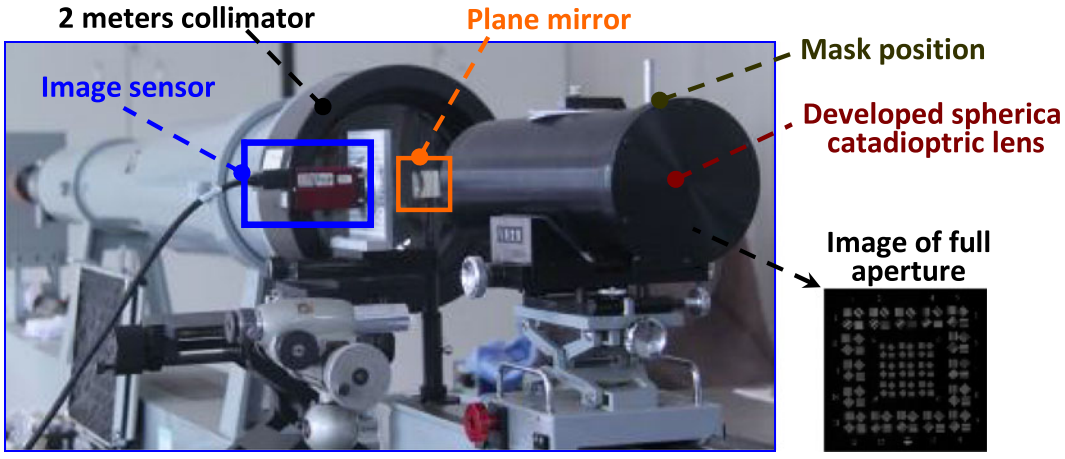

Fig. 5. The image experimental device of annulus-sector optical lens.

We used a plane mirror to turn the light, which is to reduce the length of optical system and facilitate the placement of CCD sensors.

Three different annular-sector mask structures are adopted by linear cutting, named in the way of N-d-α, Here, N is the pieces of segmented primary mirror, d is the inner diameter of mask structure and α is the angle of segmented primary mirror. Fig. 6 shows the processed mask structures, the structure parameter of Fig. 6(a) is 3-30-60° with width-diameter ratio is 0.35, Fig. 6(b) is 4-70-60° with width-diameter ratio is 0.15 and Fig. 6(c) is 4-80-80° with width-diameter ratio is 0.1,respectively. Fig. 4(b) shows the MTF comparison between the designed and tested of three different mask structures. We can see that the MTF value changes a little for it is low-sensitive to tolerance. The mask structures are placed in the location of primary mirror when imaging simulation as shown in Fig. 5.

We can get the image of full aperture optical system by placing the No. 3 standard resolution plate before the light source of collimator. Result shows that it can distinguish the line of unit 21.

The application of annulus-sector mask structures reduced the area of light, the image brightness would be accordingly drops. As a consequence, the integral time of CCD sensor ought to be adjusted to improve image quality. However the image noise also should be concerned at the same time which directly affects the quality of reconstructed images.

We present blurred images of three different annulus-sector mask structures in Fig. 6. We can see that when the 3-30-60° mask structure is used, the resolution of corresponding image is reduced,

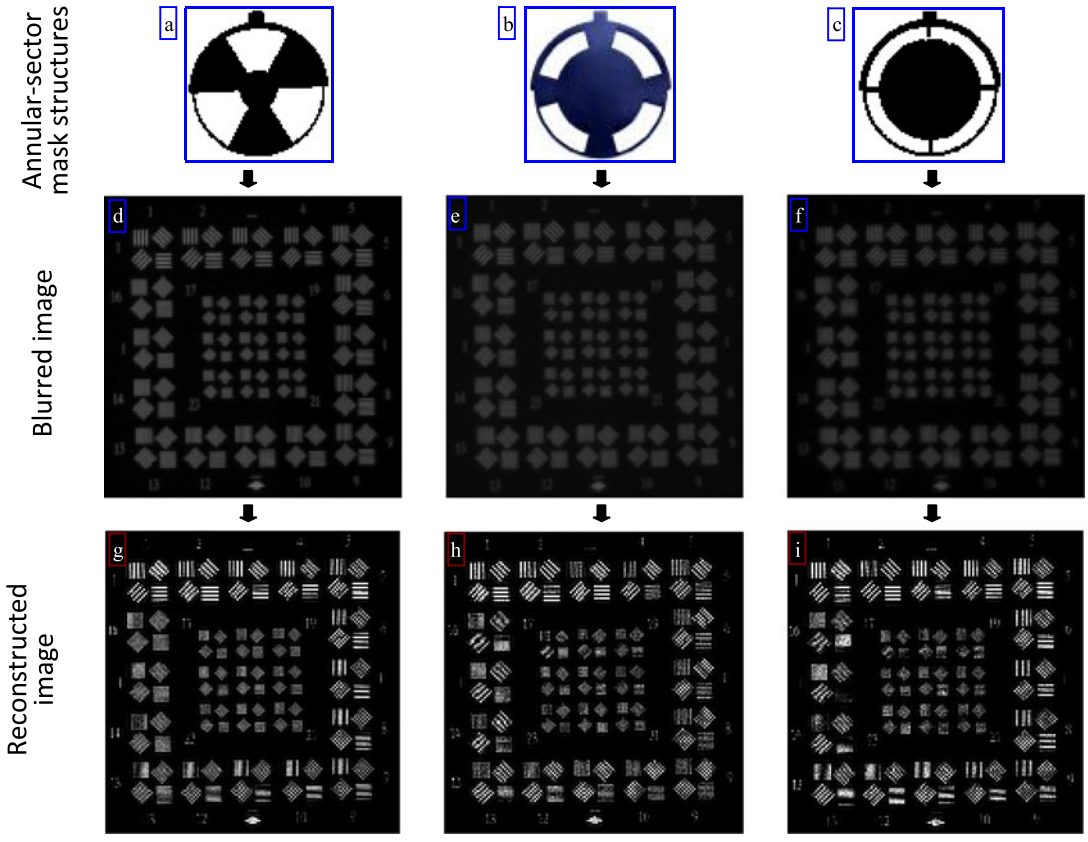

Fig. 6. Three annulus-sector structures and image results.

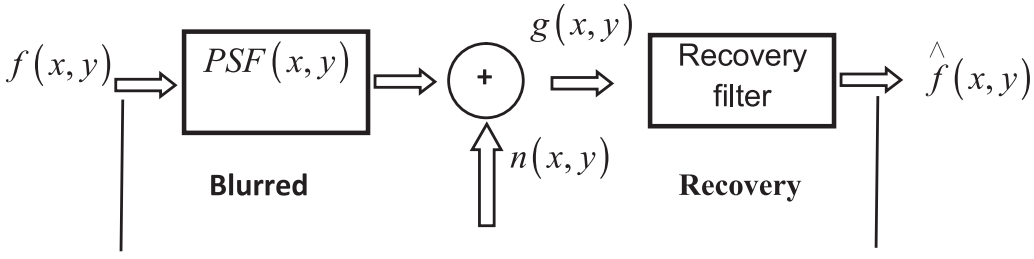

Fig. 7. The process of blurred and recovery.

which can distinguish the line of unit 17; the image of 4-70-60° mask structure can distinguish the line of unit 16; the image of 4-80-80° mask structure can distinguish the line of unit 16.

We used MATLAB for solving all the computational problems. Fig. 7 shows the process of image blurred and recovery. Here, $f(x, y)$ is original image, $PSF(x, y)$ is point spread function, $n(x, y)$ is the additive noise during the imaging process, $g(x, y)$ is the blurred images by convolution of $f(x, y)$ and $PSF(x, y)$ as well as the noise pollution. By the image restoration algorithms in MATLAB, the reconstructed image $\hat{f}(x, y)$ can be successful received.

The resolution of three reconstructed images by Lucy Richardson algorithm improved significantly, the reconstructed image of 3-30-60° mask structure can distinguish the line of unit 21 both in horizontal and vertical direction; the reconstructed image of 4-70-60° mask structure can distinguish the line of unit 20 in vertical direction and the line of unit 21 in horizontal direction; the reconstructed image of 4-80-80° mask structure can distinguish the line of unit 20 both in horizontal and vertical direction.

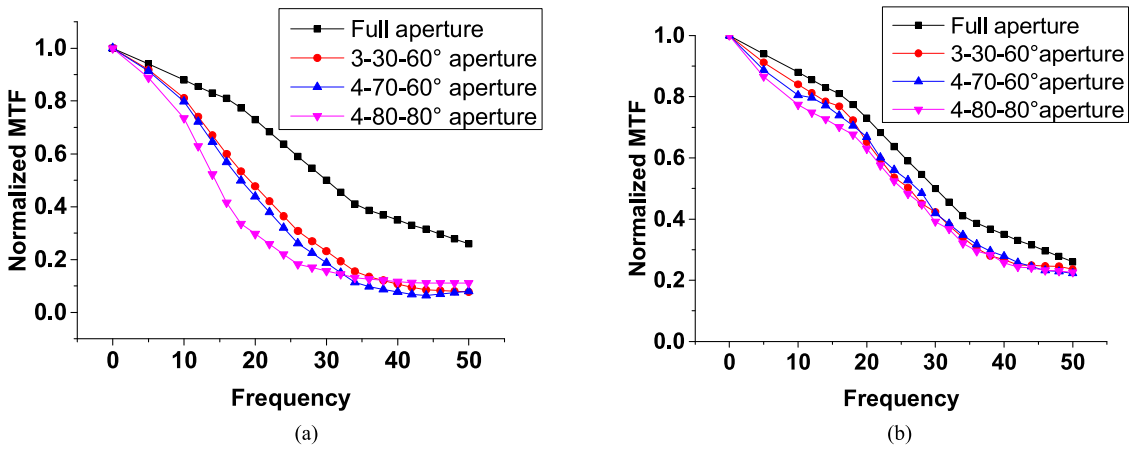

Fig. 8. MTF contrast of annulus-sector optical system and full aperture. (a) MTF contrast before restoration. (b) MTF contrast after restoration.

Fig. 8(a) shows the MTF contrast of full aperture and three annulus-sector mask aperture before reconstruction, from the results, the application of annulus-sector mask aperture greatly reduced the MTF at medium frequency, however, the MTF value can be restored to approximately that of full aperture and up to 0.23(50 lp/mm)[see Fig. 8(b)].

4. Discussions and Conclusions

The main idea in this paper is to analyze the feasibility and image properties of annulus-sector segmented primary mirror, therefore the influence of phase error and position error are not discussed here. The optical properties of annulus-sector structures are characterized by different structure parameters, and the image performance is also investigated by image experiment. The results indicate that the spatial resolution of annulus-sector optical system is lower than that of full aperture and the resolution ability is related to the annulus-sector structure. However, the resolution ability can be largely restored and close to that of full aperture by digital filtering restoration with light weight. The design results in this paper also can give guidance to the design of annulus-sector structures. It has obvious advantages in practical application.

Acknowledgment

X. X. Wei would like to thank his Supervisor, Prof. X. Ming-Qiu, academician of China National Engineering Research Institute. He will be remembered forever.

References

[1] H. P. Stahl, "JWST mirror technology development results," *Proc. SPIE*, vol. 6671, 2007, Art. no. 667102.
[2] H. P. Stahl, "JWST lightweight mirror TRL-6 results," in *Proc. IEEE Aerosp. Conf.*, Mar. 2007, pp. 1–12.
[3] Y. P. Feenix, J. H. Burge, R. Zehnder, and Y. Wang, "Fabrication and alignment issues for segmented mirror telescopes," *Appl. Opt.*, vol. 43, no. 13, pp. 2632–2642, 2004.
[4] D. G. MacMynowski and M. Björklund, "Large Aperture Segmented Space Telescope (LASST): Can we control a 12 000 segment mirror?" in *Proc. Amer. Control Conf.*, 2011, pp. 438–443.
[5] G. T. van Delle, A. B. Meinel, and M. P. Meinel, "The scaling relationship between telescope cost and aperture size for very large telescopes," *Proc. SPIE*, vol. 5489, pp. 563–570, 2004.
[6] F. Wu, Q. Wu, and Q. Lin, "Analysis of the characteristics of the Golay3 multiple-mirror telescope," *Appl. Opt.*, vol. 48, pp. 643–652, 2009.
[7] C. Xinyang, "Some key techniques of Fizeau-type optical aperture synthesis telescopes," PhD thesis, The Shanghai observatory of the Chinese academy of sciences, 2006.
[8] D. F. Robert, T. A. Tantalo, R. C. Jason, and A. M. James, "Image quality of sparse-aperture designs for remote sensing," *Opt. Eng.*, vol. 41, pp. 1957–1969, 2002.

[9] V. Vaitheeswaran, P. Hinz, G. Brusa, D. Miller, and T. Stalcup, "A PC based wave front reconstructor for MMT-AO," *Proc. SPIE*, vol. 7019, 2008, Art. no. 70190E.
[10] E. A. Bendeka *et al.*, "Status of the 6.5 m MMT telescope laser adaptive optics system," *Proc. SPIE*, vol. 77360, 2010, Art. no. 77360.
[11] H. Changyuan, "Progress in space optics and wavefront sensing technique," *Chin. J. Opt. Appl. Opt.*, vol. 1, no. 1, pp. 13–24, 2008.
[12] P. Deshmukh, D. S. Mishra, P. Parihar, and Vedashree, "Primary mirror active control system simulation of prototype segmented mirror telescope," in *Proc. Indian Control Conf.*, 2017, pp. 364–371.
[13] N. Wallace, "A concept for very large telescopes using pupil plane correction optics and lower-cost spherical primary mirror segments," 2000.
[14] K. ShengZhang, X. W. Fan, C. Li, and K. Liu, "Design and wavefront sensing for the segmented spherical primary optical telescope," in *Proc. Int. Conf. Electron. Mech. Eng. Inf. Technol.*, 2011, vol. 7, pp. 3828–3831.
[15] W. Zhongsheng and Z. Xuejun, "Symmetry of pupil in spatial synthetic aperture imaging optical system," *Opt. Precis. Eng.*, vol. 19, no. 9, pp. 1999–2005, 2011.
[16] Y. Dai, Z. Liu, Z. Jin, J. Xu, and J. Lin, "Active control of a 30 m ring interferometric telescope primary mirror," *Appl. Opt.*, vol. 48, no. 4, pp. 664–671, 2009.
[17] Z. Yimo, "Applied optics," Publishing house of electronics industry, Beijing, 2008.